

Investigation of copper corrosion behavior in chloride bath for nickel electrodeposition

Amira Gharbi^{*}, Youcef Hamlaoui²

¹ Chemical engineering Department, Physics of Matter and Radiation Laboratory LPMR, Mohamed Chérif Messaadia university, Souk Ahras 41000 Algeria.

² Chemical engineering Department, Physics of Matter and Radiation Laboratory LPMR, 1 Mohamed Chérif Messaadia university, Souk Ahras 41000 Algeria.

* amira.gharbi@univ-soukahras.dz

(Received: 24 April 2023, Accepted: 18 May 2023)

(DOI: 10.59287/ijanser.713)

(1st International Conference on Recent Academic Studies ICRAS 2023, May 2-4, 2023)

ATIF/REFERENCE: Gharbi, A. & Hamlaoui, Y. (2023). Investigation of copper corrosion behavior in chloride bath for nickel electrodeposition. *International Journal of Advanced Natural Sciences and Engineering Researches*, 7(4), 259-264.

Abstract – The present study is devoted to the electrodeposition of nickel layers on copper substrates by cyclic voltammetry from chloride bath at a scan rate of 20 mV/s and at different bath temperatures between 25 and 55 °C and then after to their corrosion behavior in chloride bath. The electrochemical behavior and corrosion properties were evaluated by cyclic voltammetry, potentiodynamic and electrochemical impedance spectroscopy. While the surface analysis of nickel coating at different temperatures was conducted by optical microscopy and white light interferometer (WLI). The obtained results show that the Ni layers have been deposited successfully on the Cu substrates. It was found that raising the bath temperature to 55 °C leads to smoother, dense, compact and recovering Ni coatings with a grain size of 0.024 nm and 0.294 μm as average roughness, which is mainly due to Ni grain refinement. While the effect of increasing bath temperature leads to a decrease in the corrosion resistance of copper.

Keywords – Nickel Coating ; EIS ; Cyclic Voltammetry ; WLI ; Grain Size

I. INTRODUCTION

Due to its wide use in several applications and requirements as in electrical connector contact and thermal nuclear energy fields due to its high thermal conductivity, excellent electrical conductivity and good workability copper has been extensively investigated [1]. However, it's considered an active metal susceptible to corrosion in humid conditions namely in the presence of chloride anions, which generally results in premature failure of copper products. Therefore several solutions have been developed to inhibit the oxidation and corrosion of

copper substrate where the most effective methods is surface coating treatment [2]. Electroplated coatings are employed in industry to improve appearance of surfaces, to provide better corrosion protection, to improve wear resistance by hard facing and sometimes to provide good electrical and thermal contacts.

On other hand, Nickel electroplating is a commercially important and useful surface finishing process. Nearly one million metric tons of nickel in the form of metals and salts are consumed annually for electroplating and other applications. The main

applications of nickel electroplating are decorative, functional and electroforming. Electrodeposited nickel coatings find use in functional applications to improve corrosion resistance, hardness, wear, magnetic and other properties. Nickel coatings are used as diffusion barriers beneath precious metal deposits in electronic applications, while nickel electroplating is common in the production of batteries [3].

The bath temperature will accelerate the diffusion rate of metal ions. Although it is well known that the bath temperature affects various properties of the electroplated layers where its effect is remains to be thoroughly investigated namely on the electrochemical behaviors, the surface morphology and the hardness of electroplated Ni layers on Cu substrates [4].

The current work aims to investigate the mechanism of Ni layers formation on Cu substrates, and the corrosion resistance of copper at different temperatures of the electrolyte containing nickel chloride and boric acid. The effect of the electrolyte temperature on the electroplated Ni layers were assessed using optic microscopy and with light interferometer (WLI).

II. MATERIALS AND METHOD

A. Materials

A Chloride bath containing nickel chloride $\text{NiCl}_2 \cdot 6\text{H}_2\text{O}$ (45 g/L) Biochem Chemopharma, and Boric acid H_3BO_3 (40 g/L) Sigma – Aldrich Canada, as a buffering agent ($\text{pH} = 3.3 \pm 0.1$), was used for electrodeposition of Ni coatings. Before electroplating, the electrolyte solution with 100 mL was stirred for a stirring speed of 150 rpm for 1 h to achieve homogeneity. The temperature of the electrolyte solution was maintained at 25, 35, 45 and 55°C during electroplating. Copper substrate were used as working electrode with chemical composition as shown in Table 1). Before each experiment, the surface of the substrates is polished using silicon carbide (SiC) abrasive papers from 180 up to 2500, cleaned ultrasonically for 4 min with ethanol, and then rinsed with water and immediately dried with hot pulsed air.

Table 1. Chemical composition of (wt%) of copper

Element	Cu	Ni	Zn	Fe	Mn	Se	Pb	Sn	Bi
wt%	99.29	<0.00	0.14	0.07	0.02	<0.00	0.03	<0.00	0.02

B. Cathodic electrodeposition and electrochemical tests:

Electroplating was done in a three-electrode cell configuration equipped with a Platinum wire (Pt) as Counter Electrode (CE), copper with an active surface area of 0.785 cm^2 as cathode electrodes and saturated calomel $\text{Hg}/\text{Hg}_2\text{Cl}_2$ as reference Electrode (RE). The electrodes were dipped in chloride bath. A computerized potentiostat/galvanostat (BIOLOGIC 150) driven by ECLab software. Potentiodynamic polarization curves were obtained at a scan rate of 1 mV/s, The cyclic voltammetry curves were obtained at a scan rate of 20 mV/s between 0.1 and -1.2 V. The impedance data were recorded at the corrosion potential (E_{corr}) between 500 kHz and 10 MHz at 10 mV as the applied sinusoidal perturbation. The EIS results were fitted using Zview software.

C. UV- visible spectrophotometry

UV-visible spectrophotometry is a method used routinely for the study of solutions containing metal ions because their electronic transitions correspond to wavelengths in the UV/visible range. Verification and analysis of the existence of nickel was verified using a UV-visible SECOMAM® spectrophotometer. The liquid sample is placed in a quartz cell in the measurement compartment of the spectrophotometer in the path of the incident beam.

III. RESULTS

The corrosion current density increase (I_{corr}) with increasing bath temperature from 25°C to 55°C.

Fitting results of EIS diagrams of copper in chloride bath shows that increasing bath temperature reduce the charge transfer resistance “ R_{ct} ” of the material from 354.4 to 14.03 $\Omega \cdot \text{cm}^2$.

The cyclic voltammograms clearly show that the cathodic overpotential increases towards more positive values with increasing solution temperature.

The decrease in roughness values can be attributed to the formation of a thin or homogeneous film on the surface of the substrate.

The most intensive Ni (II) peak at was at 395 nm.

IV. DISCUSSION

A. Polarization resistance

In order to investigate the corrosion behaviour of copper in nickel electroplating bath, potentiodynamic polarization measurements with a scan rate of 1 mV/s was conducted. The potentiodynamic polarization curves of copper in chloride bath are shown in Figure 1 and the electrochemical corrosion parameters derived from these curves are gathered in Table 2. The corrosion potential (E_{corr}) values polarization resistance (R_p), anodic and cathodic Tafel slopes (β_a and β_c) and corrosion current density (I_{corr}) were estimated from the intersection of linear portions of anodic and cathodic curves of the Tafel plots. the polarization resistance R_p was calculated by Stern-Geary equation (Equation 1) [5]:

$$R_p = \frac{\beta_a \cdot \beta_c}{2.3 \cdot I_{corr} \cdot (\beta_a + \beta_c)} \quad (1)$$

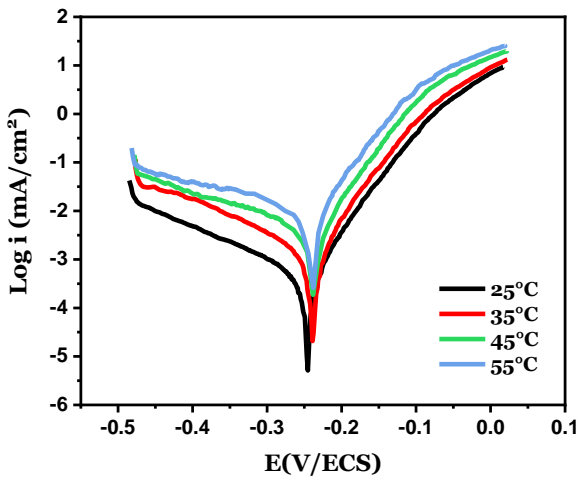


Fig. 1 Potentiodynamic polarization curves obtained on copper substrate in chloride bath at different temperatures.

It can be seen from Figure 1 that the corrosion current density increase (I_{corr}) with increasing bath temperature from 3.074 at 25°C to 47.348 $\mu\text{A}\cdot\text{cm}^{-2}$ at 55°C; while the corrosion resistance of copper decreased which is due both to the increase of Cl^- activity [6] and to the oxygen diffusion toward the metal surface. It is noted that the oxygen content of the water directly affects the corrosion rate since it the solubility decreased with increasing temperature [7].

Table 2. Potentiodynamic polarization curves obtained on copper substrate in chloride bath at different temperatures.

T (°C)	E_{corr} vs. SCE/mV	I_{corr} ($\mu\text{A}\cdot\text{cm}^{-2}$)	β_a (mV)	β_c (mV)	R_p ($\Omega\cdot\text{cm}^{-2}$)
25°C	-245.781	3.074	69.5	226.1	7518.81
35°C	-238.577	7.158	73.9	216.6	3346.86
45°C	-237.081	20.568	79.4	413.0	1407.77
55°C	-239.392	47.348	88.8	785.7	732.62

B. Electrochemical impedance spectroscopy

The EIS measurements were carried out in the chloride bath at different temperatures in the frequency range between 500 kHz and 10 MHz to obtain further mechanistic information, depending on the different parameters imposed on the system. The samples were kept immersed in the test solution for 30 min before starting the test to attain the steady state of the potential. Nyquist diagrams are presented in Figure 2.

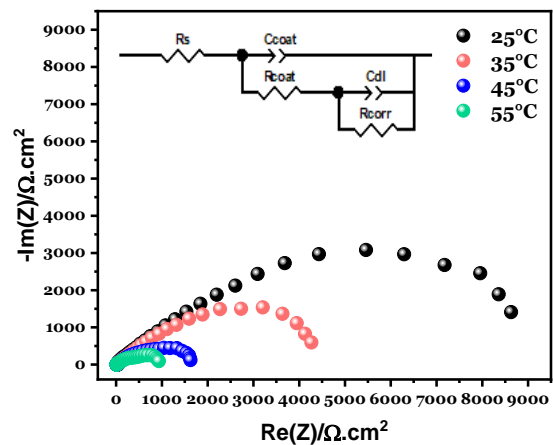


Fig. 2 EIS diagrams (Nyquist plot) of copper in chloride bath at different temperatures.

The EIS plots in Figure 2 were analysed using the Zview software with a proposed equivalent electrical circuit which fit best the EIS diagrams. The Nyquist curves show the existence of two capacitive loops associated to 2 relaxation times. The fitting values obtained for the elements of the equivalent electric circuit for copper in chloride bath are gathered in Table 3. It can be seen that when the bath temperature increase, the polarization resistance calculated at low frequencies gradually decreased. Indeed, the increase in temperature led to a reduction in the resistance which slow down the

movement of the aggressive ions, therefore reducing the corrosion resistance of the material. Thus, the temperature seems to affect the mobility of Cl⁻ in the solution, which, in turn, affects the corrosion resistance [6].

Table 3. Fitting results of EIS diagrams of copper in chloride bath.

T (°C)	25°C	35°C	45°C	55°C
Rs (Ω.cm²)	13.84	11.1	9.74	7.21
CPEdc μFs⁽ⁿ⁻¹⁾ cm⁻²	43.27	108.0	7.244	39.75
ndc	0.83	0.75	0.99	0.91
Rtc (Ω.cm²)	354.4	166.1	21.89	14.03
CPEc (mFs⁽ⁿ⁻¹⁾cm⁻²)	0.233.10 ⁻³	0.422	0.590	0.61
nc	0.61	0.61	0.55	0.61
Rc (Ω.cm²)	8313	4066	1464	479.9
CPE₃ (mFs⁽ⁿ⁻¹⁾ cm⁻²)	-	-	-	6.54
N₃	-	-	-	1
R₃ (Ω.cm²)	-	-	-	259.3

C. Cyclic voltammetry

In order to select the suitable potential for electrodeposition, d.c polarisation measurements were performed. The influence of electrolyte temperature on the polarisation curve for Ni on copper substrate in chloride bath is shown in Figure 3. The voltametric scans were started from 0.1 to -1.2 V vs. SCE at a scan rate of 20 mV/s.

According to Figure 3, cyclic voltammograms are characterized by the presence of one cathodic peak and an anodic one. When the scan is performed towards negative potentials, the cathodic current increases sharply once a nucleation phenomenon begins [8]. It's well observed that the cathodic current starts at about -0.65 V vs SCE which is associated to Ni nucleation and reduction. Moreover, the cathodic overpotential increases towards more positive values with increasing solution temperature where a higher cathodic overpotential decreases the energy of the nucleus formation, leading to an increase in the nucleus densities and a decrease in the crystallite size [9]. Then the current increases sharply when the sweep continues towards more negative potentials, corresponding to a deposit of nickel with metallic grey deposits and an H₂ co-evolution [10].

As the potential shifts further to the cathodic values, the increase in corresponding cathodic is

related to the increase in the density nuclei and the crystal growth [8]. The H₂ co-evolution became visible with the formation of H₂ gas bubbles at the edges of the deposited layer on the surface of the electrode beyond -1.0 V vs. SCE [10]. Respectively, hydrogen bubbles began to aggregate on the electrode. This phenomenon indicates that the Ni deposition is accompanied by the evolution of hydrogen gas which seems to deteriorate the quality of nickel deposited coating by the formation of a dendritic or porous deposit [11].

Additionally, on the voltammograms, it can be seen the presence of crossovers of the cathodic and anodic branches, which is typically associated with the formation of a new phase, involving a nucleation and growth process [12].

Then the oxidation peak of Ni deposit was more apparent once the reversed potential was shifted to more negative values at around -0.1 V [11]. It is noted that the electrodeposition process of nickel on copper by cyclic voltammetry according to the following reactions:

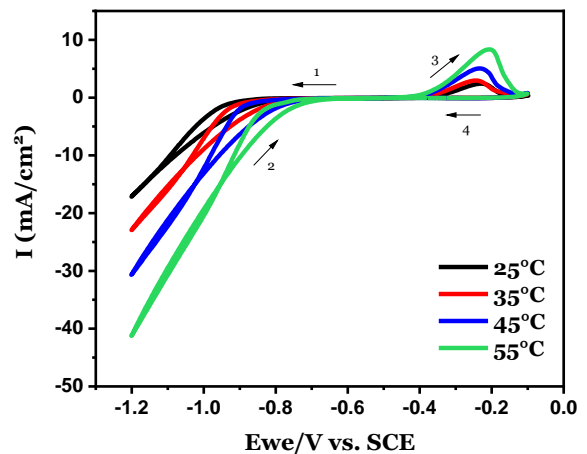


Fig. 3 Cyclic voltammograms of Ni plating on Cu electrode from chloride bath.

D. Surface morphology

The influence of temperature on the surface morphology of the coating surface is displayed in Figure 4. It can be observed that increasing the temperature leads to smoother dense, compact and recovering Ni coatings, unlike those at 25,35,45°C with impurities and pitting in the coating. This may be due to the soluble iron which cause hazes or

pitting and a reduction in ductility. To confirm this behaviour, the surface morphology of the samples was examined by a white light interferometer (WLI) measurement and the results are presented in 3D images as shown in Figure 5 and the calculated parameters of the film are gathered in Table 4.

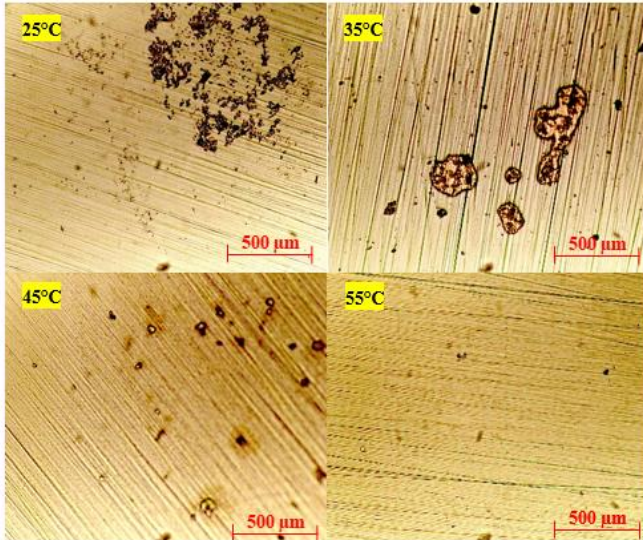


Fig. 4 Optical images ($\times 500$) of the deposits obtained at different temperatures from chloride bath.

The WLI images clearly show that the average thickness of the film decreases with increasing bath temperature. It is also noticed that the darker the colour of the area or spots in the 3D images, the thinner the deposit, and the black areas are thus attributed to the surface of the substrate [13].

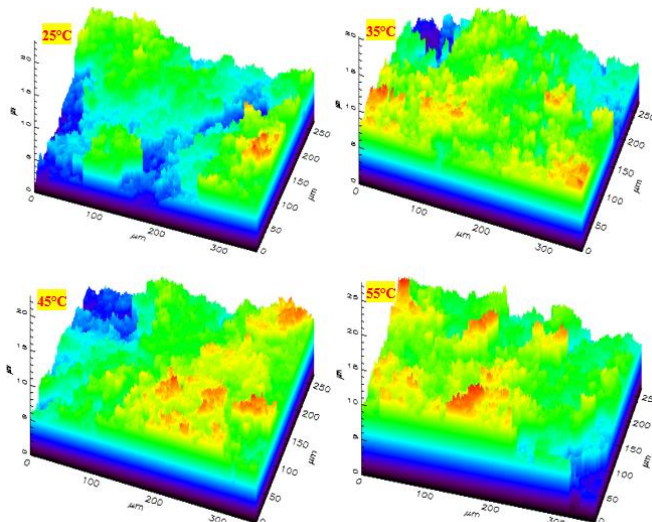


Fig. 6 EIS diagrams (Nyquist plot) of copper in chloride bath at different temperatures.

The WLI images clearly show that the films produced at 55°C exhibit greater uniformity, less

roughness, and a finer grain size than the films obtained at 25, 35 and 45 °C.

The decrease in roughness values calculated with the FRT Mark III software (Table 4) can be attributed to the formation of a thin or homogeneous film on the surface of the substrate. Moreover, the values found corroborate the advantage of increasing bath temperature to obtain films that exhibit less roughness and a decrease in grain size. This contributes to obtain plates with a greater compaction degree [14].

Table 4. Surface parameters of nickel coating obtained on copper from chloride bath at different bath temperatures

T (°C)	Average thickness (µm)	Grain size (nm)	Roughness (µm)
25°C	3.241	0.055	0.483
35°C	4.795	0.045	0.437
45°C	5.509	0.038	0.363
55°C	7.043	0.024	0.294

E. UV- visible spectrophotometry

The UV-Vis spectra recorded of chloride bath solution (H_3BO_3 and $NiCl_2$) compared to the blank solution (H_3BO_3) is shown in figure 7.

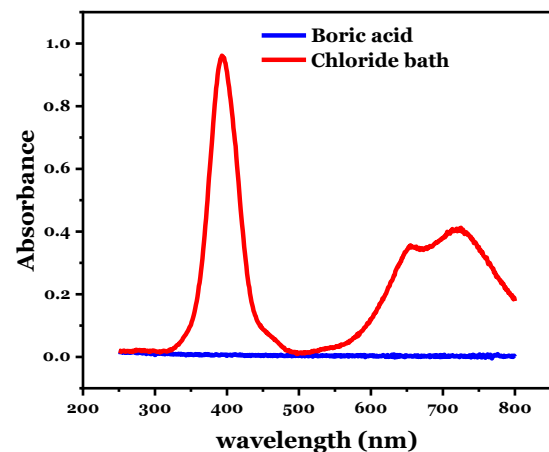


Fig. 7 UV-Vis spectra of boric acid and chloride bath.

It can be seen from the recorded spectra two absorption peaks at 395 and 730 nm related to Ni (II) and a shoulder at 655 nm related to the $[Ni(H_2O)_6]^{2+}$ octahedral ion. [15]

V. CONCLUSION

The Ni layers have been performed successfully on the Cu alloy substrates at various electrolyte temperatures. The bath temperatures influence the surface morphology of Ni coatings and the electrochemical behaviour of Cu.

The corrosion current density (I_{corr}) of copper in chloride bath increases with increasing bath temperature from 3.074 at 25°C to 47.348 $\mu\text{A}\cdot\text{cm}^{-2}$ at 55°C.

The coating surface parameters estimated by white light interferometry show that by increasing the bath temperature to 55°C, the average thickness of the coating increases from 3.241 μm to 7.043 μm , while the surface roughness and the grain size decreases which leads to a greater compaction degree, thin and homogeneous film.

It was found that 55°C represents the optimal bath temperature for nickel electrodeposition.

REFERENCES

- [1] WAN, Ye, WANG, Xiumei, SUN, Hong, et al. Corrosion behaviour of copper at elevated temperature. *Int. J. Electrochem. Sci*, 2012, vol. 7, no 9, p. 7902-7914.
- [2] BALAJI, J. et SETHURAMAN, M. G. Improved corrosion resistance by forming multilayers over a copper surface by electrodeposition followed by a novel sol-gel coating method. *RSC advances*, 2016, vol. 6, no 98, p. 95396-95404.
- [3] TUCK, J. R., KORSUNSKY, Alexander M., DAVIDSON, R. I., et al. Modelling of the hardness of electroplated nickel coatings on copper substrates. *Surface and Coatings Technology*, 2000, vol. 127, no 1, p. 1-8.
- [4] SUSETYO, Ferry Budhi, FAJRAH, Musfirah Cahya, et SOEGIJONO, Bambang. Effect of electrolyte temperature on properties of nickel film coated onto copper alloy fabricated by electroplating. *e-Journal of Surface Science and Nanotechnology*, 2020, vol. 18, p. 223-230.
- [5] STERN, Milton et GEARY, Al L. Electrochemical polarization: I. A theoretical analysis of the shape of polarization curves. *Journal of the electrochemical society*, 1957, vol. 104, no 1, p. 56.
- [6] LI, Qiannan, ZHANG, Yifan, CHENG, Yulin, et al. Effect of Temperature on the Corrosion Behaviour and Corrosion Resistance of Copper-Aluminium Laminated Composite Plate. *Materials*, 2022, vol. 15, no 4, p. 1621.
- [7] BENTISS, Fouad, OUTIRITE, Moha, TRAISNEL, Michel, et al. Improvement of corrosion resistance of carbon steel in hydrochloric acid medium by 3, 6-bis (3-pyridyl) pyridazine. *Int. J. Electrochem. Sci*, 2012, vol. 7, no 2, p. 1699-1723.
- [8] SAHARI, A., AZIZI, A., SCHMERBER, G., et al. Nucleation, growth, and morphological properties of electrodeposited nickel films from different baths. *Surface Review and Letters*, 2008, vol. 15, no 06, p. 717-725.
- [9] FENG, Lu, REN, Yong-Yue, ZHANG, Yan-Heng, et al. Direct correlations among the grain size, texture, and indentation behaviour of nanocrystalline nickel coatings. *Metals*, 2019, vol. 9, no 2, p. 188.
- [10] JAMIL, Zadariana, RUIZ-TREJO, Enrique, et BRANDON, Nigel P. Nickel electrodeposition on silver for the development of solid oxide fuel cell anodes and catalytic membranes. *Journal of The Electrochemical Society*, 2017, vol. 164, no 4, p. D210.
- [11] DI BARI, George A. Electrodeposition of nickel. *Modern electroplating*, 2000, vol. 5, p. 79-114.
- [12] BOUBATRA, Mustapha, AZIZI, Amor, SCHMERBER, Guy, et al. The influence of pH electrolyte on the electrochemical deposition and properties of nickel thin films. *Ionics*, 2012, vol. 18, p. 425-432. WAN, Hongjun, SONG, Qiushi, SHAN, Changlu, et al. Microstructural modification of Ni electrodeposit in an acidic NiCl₂ solution. *Journal of Electroanalytical Chemistry*, 2020, vol. 873, p. 114349.
- [13] ROUABHIA, F., HAMPLAOU, Y., MEROUFEL, Abdelkader, et al. Corrosion properties of ceria-based coating electrodeposited from alkaline bath on electrogalvanized steel. *Journal of Applied Electrochemistry*, 2021, vol. 51, p. 567-580.
- [14] APERADOR CHAPARRO, William Arnulfo et LOPEZ, Enrique Vera. Electrodeposition of nickel plates on copper substrates using PC y PRC. *Matéria (Rio de Janeiro)*, 2007, vol. 12, p. 583-588.
- [15] VOSHKIN, Andrey A., ZAKHODYAEVA, Yulia A., et ZINOV'EVA, Inna V. "Green" Extractants in the Recovery Processes of Non-ferrous Metal Ions from Technological Solutions. *KnE Materials Science*, 2020, p. 227-238-227-238.